

Mesoscale variability in the metabolic balance of the Sargasso Sea

Beatriz Mouriño-Carballido¹ and Dennis J. McGillicuddy Jr.

Applied Ocean Physics & Engineering, Woods Hole Oceanographic Institution, Woods Hole 02543, Massachusetts

Abstract

Net community production (NCP) experiments based on *in vitro* changes in dissolved oxygen were carried out in three mesoscale eddies investigated in the Sargasso Sea in the summer of 2004. NCP estimates ranged from negative to positive values, and the age and type of the sampled eddy were important factors responsible for this variability. Positive rates occurred in younger cyclones and in areas of eddy-eddy interactions, whereas negative NCP rates were observed in anticyclones and older cyclone features that were decaying. This information was combined with a nine-year data set from the BATS program and satellite altimeter data to assess the role of mesoscale eddies in the metabolic balance of the Sargasso Sea. Indirect NCP estimates (NCPe) were obtained by calculating the difference between ¹⁴C phytoplankton production and bacterial carbon demand rates. The results showed highly variable NCPe rates that spanned the range of direct NCP observations.

The metabolic balance of the photic layer in the ocean is determined by net community production (NCP), the difference between gross primary production (GPP) and total respiration (R). An excess of production over respiration, referred to as net autotrophic metabolic balance, implies a net synthesis of organic carbon that can be exported either vertically to the deep ocean, laterally to other regions, or to higher trophic levels. A negative balance, referred to as net heterotrophic balance, represents a net demand for allochthonous supplies of organic carbon or the consumption of dissolved organic matter produced elsewhere. Thus, the determination of NCP constitutes an important step in understanding carbon budgets and global change predictions.

The Winkler technique has been used for over 70 years to estimate plankton photosynthesis and respiration rates based on *in vitro* changes in dissolved oxygen. However, when compared with the method to measure phytoplankton carbon incorporation rates based on ¹⁴C uptake, this technique is a laborious and time-consuming procedure

(Williams and Jenkinson 1982), which has severely hampered the development of a global database.

Research efforts have been focused on building empirical regional-scale GPP : R relationships in order to predict NCP. The contradictory results obtained thus far have opened debate about the net metabolic state of the open ocean, *i.e.*, whether the open ocean as a whole is in equilibrium or slightly autotrophic metabolic balance (Williams 1998) versus the net metabolic balance being heterotrophic (Duarte *et al.* 1999). In recent years, an intense effort has been made to address and investigate this enigmatic discrepancy. A number of studies using local-scale measurements of net oxygen production and respiration carried in the NE subtropical Atlantic, in different seasons and geographical locations, have repeatedly reported a net heterotrophic balance of the photic layer (Serret *et al.* 2002). The only study published to date that describes seasonal changes in the metabolic balance of a subtropical oligotrophic site, based on *in vitro* changes in oxygen concentration, reported net heterotrophy throughout the year at station ALOHA in the subtropical Pacific (Williams *et al.* 2004). It has been proposed that the measured net heterotrophy could be an artifact of undersampling episodic events of net autotrophy that would be decoupled from the more constant heterotrophic processes (Karl *et al.* 2003). In the lack of measurable nutrients during the summer, Jenkins and Goldman (1985) described the development of a sub-surface oxygen maximum associated with photosynthetic production in the Sargasso Sea. Their study of the seasonal cycle of oxygen supersaturation leads to a photosynthetic oxygen production estimation of the order of 0.5 mmol m⁻² d⁻¹, which is consistent with a net autotrophic metabolic balance through the year.

One of the mechanisms that could generate pulses of net autotrophy is associated with mesoscale eddies. The suggested ecological role for mesoscale processes is not new. However, due to the costs and logistics involved in sampling high-frequency stochastic events, the knowledge about the role that these features play in the net metabolic state of open oceanic regions is scarce and limited to a few observations (Gonzalez *et al.* 2001; Fernandez *et al.* 2004; Maixandeu *et al.* 2005). A recent study conducted in the

¹Corresponding author. Present address: Departamento de Ecología e Bioloxía Animal, Universidade de Vigo, 36310 Vigo, Spain, bmourino@uvigo.es.

Acknowledgments

We thank the following individuals for their help with this research: V. Kosnyrev, W. Jenkins, P. Rowe, L. Anderson, and F. Tapia (Woods Hole Oceanographic Institution) and P. Serret and V. Pérez (University of Vigo). R. Leben (University of Colorado) provided the altimetry data that were essential for targeted sampling of eddy features described in this study. We are grateful to the participants of OC404-1 and OC404-4 cruises for their valuable support at sea and the numerous people who were involved in the collection and analysis of the Bermuda Atlantic Time Series data. We thank J. Doutré and D. Nowack for the design and construction of the temperature control system used in summer 2004. We thank N. Gruber, S. Neuer, K. Buesseler, D. Steinberg, and C. Carlson for their comments on this manuscript.

B. Mouriño-Carballido was supported by a Fulbright post-doctoral fellowship. Support of this activity by the U.S. National Science Foundation and the National Aeronautics and Space Administration is greatly appreciated.

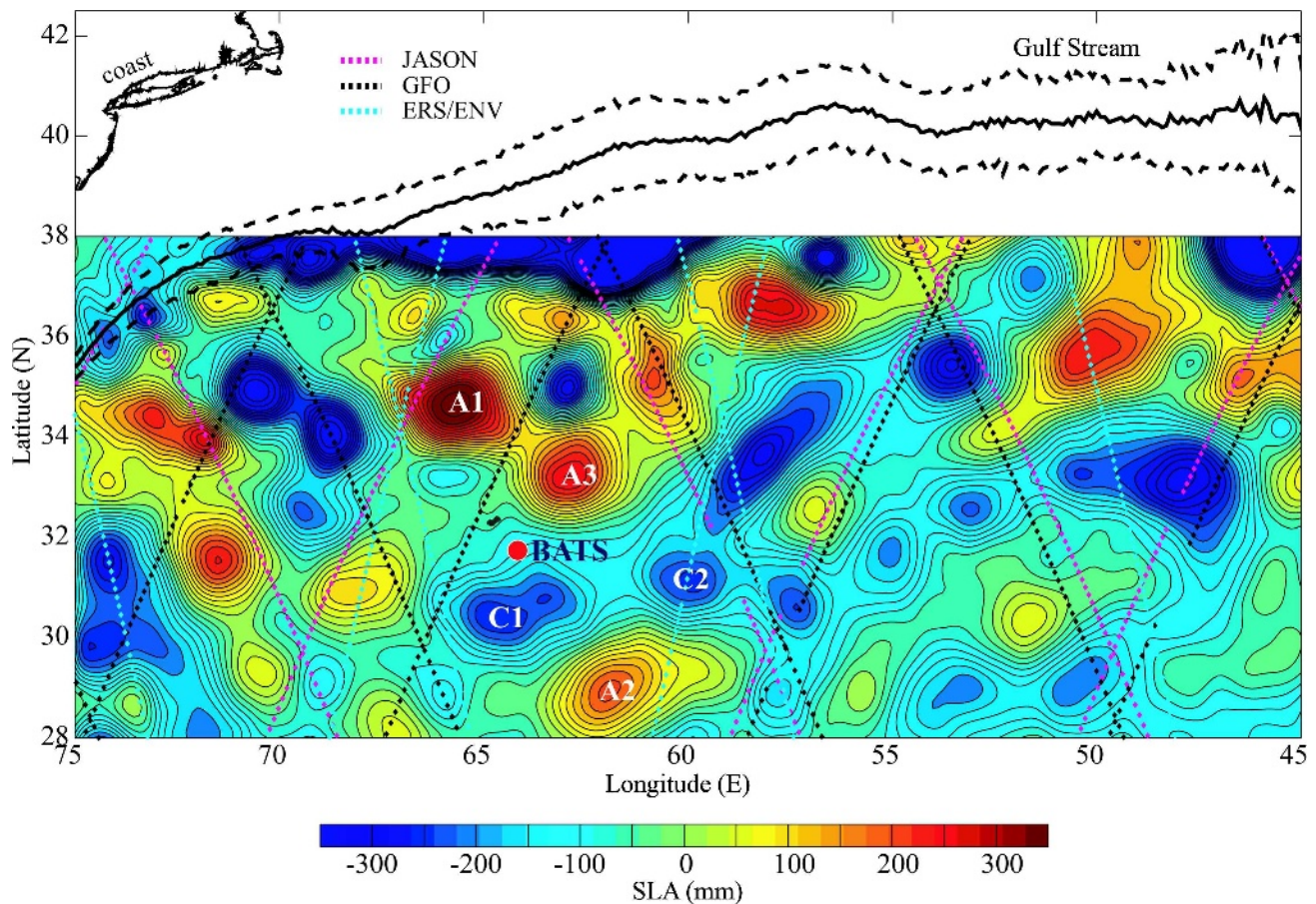


Fig. 1. Objective analysis of sea-level anomaly (SLA) (mm) for 05 June 2004 prior to the first cruise. SLA is computed relative to a long-term mean sea level, such that positive (negative) mesoscale features in SLA are associated with anticyclonic (cyclonic) eddies. The coastline is shown in black. The solid black line indicates the mean path of the Gulf Stream. The dashed lines correspond to a one standard deviation meander envelope. Cyan, pink, and black lines represent satellites passes. The five eddies features (A1, A2, A3, C1, C2) identified prior to, and tracked during, the EDDIES cruises are indicated. A1, C1, and C2 were the three eddies selected for this study. BATS, Bermuda Atlantic Time-series site.

NE subtropical Atlantic estimated that the potential enhancement of primary production rates associated with mesoscale features could be $<7\%$ of the total net primary production of the region (Mourino et al. 2005).

This observation contrasts with results obtained in the more dynamic NW Atlantic, where substantial evidence indicates that mesoscale eddies are the main mechanism that transports nutrients into the photic layer (Siegel et al. 1999).

Three different types of mid-ocean eddies have been identified in the Sargasso Sea (McGillicuddy et al. 1999): cyclones, anticyclones, and mode-water eddies (MWEs). Cyclones and MWEs tend to displace upper ocean isopycnals toward the surface, causing nutrient input into the euphotic zone. Eddy age is another important factor that controls the associated biological response (Sweeney et al. 2003). The formation and intensification phases of the eddy's lifetime occur when nutrients are transported into the euphotic layer and the associated biological response occurs (McGillicuddy and Robinson 1997).

Measurements of net oxygen production and respiration were conducted in the Sargasso Sea in summer 2004, during the first year of field work of the Eddy Dynamics, Mixing,

Export, and Species composition (EDDIES) project. Our goal was to (1) assess the spatial variability in the net metabolic carbon balance of planktonic communities associated with different kinds of eddy features, and (2) determine the temporal variability in the metabolic balance associated with two different times during the lifetime of one particular eddy. This information was combined with a nine-year data set from the Bermuda Atlantic Time Series Study (BATS) in the oligotrophic northwestern Sargasso Sea (31.7°N , 64.2°W) and altimeter satellite images in order to investigate the role of mesoscale eddies in the metabolic balance of the Sargasso Sea.

Methods

Locating and tracking mesoscale eddies—Eddy features of interest were identified prior to, and tracked during, the EDDIES cruises using near-real-time satellite altimetry measurements from TOPEX/Poseidon, Jason, Geosat Follow-On, and European Remote Sensing platforms, available through the Colorado Center for Astrodynamics Research, Northwestern Atlantic Near Real-Time Altime-

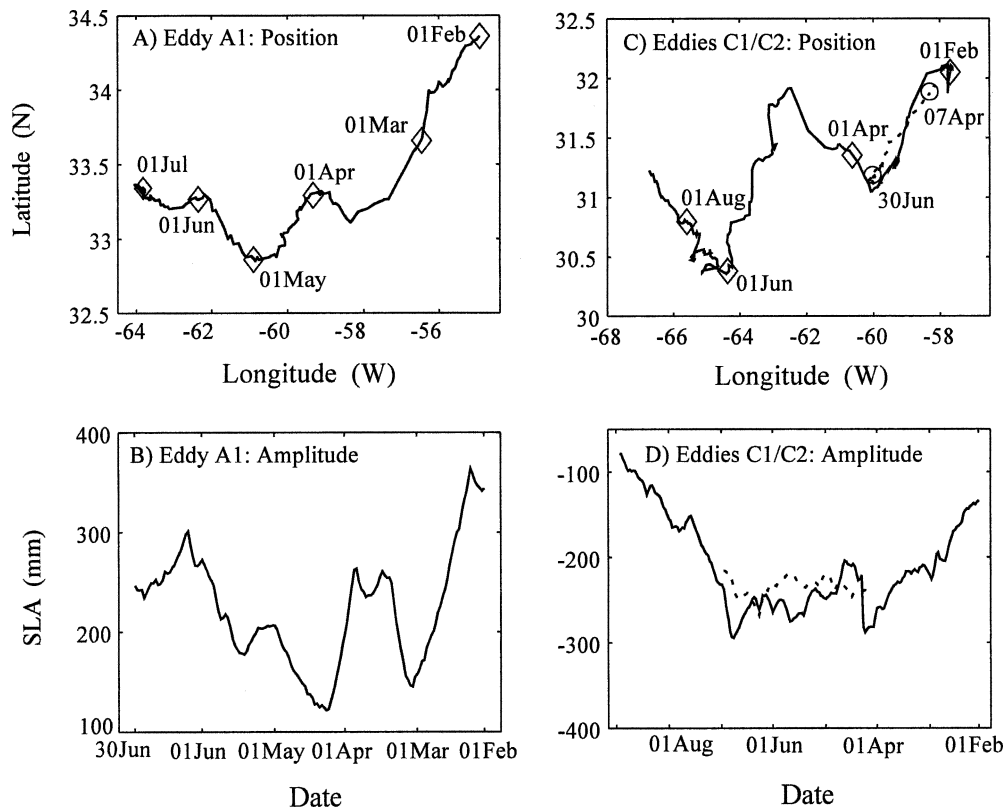


Fig. 2. Trajectories and histories of sea-level anomaly (SLA) extrema from (A, B) the anticyclonic eddy A1 and (C, D) cyclonic eddies C1 and C2 tracked in 2004. SLA is computed relative to a long-term mean sea level, such that positive (negative) mesoscale features in SLA are associated with anticyclonic (cyclonic) eddies. Dotted line represents trajectory and history of SLA for C2 from 07 April 2004 to 30 June 2004.

ter Data Viewer (<http://ccar.colorado.edu/>) and the U.S. Navy (<http://www7300.nrlssc.navy.mil/altimetry/>). Eddy statistics from previous years (<http://science.whoi.edu/users/mcgillic/tpd/anim.html>) provided some guidance with respect to expected eddy trajectories over the course of the planned field work (June–August). Three candidate eddies were selected for this study: one anticyclone (A1, centered at approx. 33.0°N, 62.9°W) and two cyclones (C1, centered at approx. 30.5°N, 64.7°W; C2, centered at approx. 31.4°N, 60.5°W) (Fig. 1). All three features were tracked in the satellite data archive to determine their trajectories and recent history of sea-level anomaly (SLA) extrema (Fig. 2). Ocean color imagery from the Moderate Resolution Imaging Spectroradiometer (MODIS) was also used to assess eddy impacts on upper ocean bio-optical characteristics.

Eddies passing near the BATS site during the 1993–2002 period were identified as in Sweeney et al. (2003). Additional confirmation of the influence of mesoscale features was made by examination of hydrographic profiles at BATS. Eddy field animations for the domain spanning latitude 28° to 38°N and longitude of 75° to 45°W are available online at <http://science.whoi.edu/users/mcgillic/tpd/anim.html>.

EDDIES cruise tracks and hydrography—Two oceanographic cruises (OC404-1, 11 June–03 July 2004; OC404-4,

25 July–03 August 2004) were conducted on board the R/V *Oceanus* in the Sargasso Sea (Fig. 3). On the first cruise, hydrographic sections across the three candidate eddies were carried out in order to select the eddy feature to be targeted and intensively sampled for the rest of the summer. C1, the selected eddy, was subjected to an intensive study during the second part of the first cruise. Then, it was reoccupied during the second cruise in order to study the temporal evolution of the biogeochemical properties associated with this water body. The BATS site, located at the edge of interaction between A1 and C1 at the time when the surveys were conducted, and initially chosen as a background reference station for summer conditions, was occupied once on each cruise. Conductivity–temperature–depth (CTD) profiles were conducted with a SeaBird 911 attached to a rosette equipped with Niskin bottles. Chlorophyll *a* (Chl *a*) concentrations determined by Turner extractions were used to calibrate the CTD fluorometer.

Net production and respiration rates based on in vitro changes in dissolved oxygen—Seven experiments were carried out to determine NCP, R, and GPP from in vitro changes in dissolved oxygen during 24-h light/dark bottle incubations (see Table 1). Water samples were collected from a 24-bottle rosette (10-dm³ PVC Niskin bottles) through silicon tubing into calibrated borosilicate glass bottles, with a nominal volume of 120 cm³. Four to five

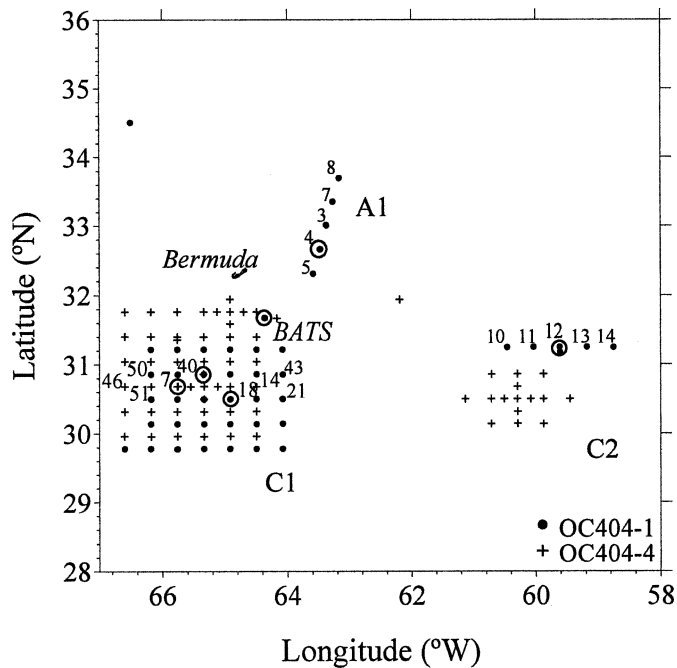


Fig. 3. Location of CTD sampling stations studied during the OC404-1 (dots) and OC404-4 (crosses) cruises in the Sargasso Sea in summer 2004. Circles around dots indicate stations where NCP experiments were conducted. Numbers represent CTD stations. A1, C1, and C2 indicate the location of anticyclonic eddy A1 and cyclonic eddies C1 and C2, respectively. BATS, Bermuda Atlantic Time-series site.

depths were chosen according to the profiles of fluorescence and photosynthetically available radiation (PAR). Samples from each depth were collected from three different Niskin bottles to minimize exchange of oxygen with the head space in the bottle. When ship logistics precluded predawn sampling, precautions were taken to minimize exposure of samples to light and temperature greater than those experienced in situ. From each depth, ten to fourteen clear and dark bottles were incubated for 24 h in a light- and temperature-controlled on-deck incubator (Mouriño et al. unpubl. data). Averaged standard deviation (STD) of incubator temperature from the target temperature for each experiment was $<0.5^{\circ}\text{C}$ (see Table 1). Five to seven replicates bottles were fixed immediately after the incubation experiments started in order to quantify the initial oxygen concentrations. Measurements of dissolved oxygen were made with an automated Winkler titration system on the basis of a potentiometric end-point detector, as described in Williams and Jenkinson (1982).

Net community production (NCP), community respiration (R), and gross primary production (GPP) rates were calculated as

$$\text{NCP}_{ij} = \overline{L_{ijz}} - \overline{I_{ijz}}$$

$$\text{R}_{ij} = \overline{I_{ijz}} - \overline{D_{ijz}}$$

$$\text{GPP}_{ij} = \overline{L_{ijz}} - \overline{D_{ijz}}$$

where L , D , and I are light and dark incubated and time zero replicates. Subscripts represent experiment number (i), depth level in each particular experiment (j), and number of replicates for each depth level in each particular experiment (z).

Standard errors associated with NCP (SENCP), R (SER), and GPP (SEGPP) were calculated as

$$\text{SER}_{ij} = \sqrt{(\text{SEI}_{ijz}^2 + \text{SED}_{ijz}^2)}$$

$$\text{SENCP}_{ij} = \sqrt{(\text{SEL}_{ijz}^2 + \text{SEI}_{ijz}^2)}$$

$$\text{SEGPP}_{ij} = \sqrt{(\text{SEL}_{ijz}^2 + \text{SED}_{ijz}^2)}$$

where SLE, SEI, and SED are standard errors of light and dark incubated and time zero replicates.

Oxygen concentration values of light and dark incubated and time zero replicates were subjected to meticulous quality control. The averaged standard errors of NCP and R rates, calculated from the quality-controlled data, were $0.15 \text{ mmol O}_2 \text{ m}^{-3} \text{ d}^{-1}$ ($n = 30$) and $0.25 \text{ mmol O}_2 \text{ m}^{-3} \text{ d}^{-1}$ ($n = 27$). These results are comparable to the averaged standard errors of NCP and R rates ($0.32 \text{ mmol O}_2 \text{ m}^{-3} \text{ d}^{-1}$, $n = 63$; $0.20 \text{ mmol O}_2 \text{ m}^{-3} \text{ d}^{-1}$, $n = 119$; respectively) reported by Robinson et al. (2002) in their study of the plankton respiration in the Eastern Atlantic Ocean using the same methodology. For comparative purposes, GPP, NCP, and R rates were integrated to the 1% light depth measured during the cruises ($\sim 100 \text{ m}$). Associated standard errors ($\text{mg C m}^{-2} \text{ d}^{-1}$) for each of the depth-integrated rates (GPP, NCP, and R) were calculated as:

$$\text{SE}_i = \sqrt{\sum_{j=1}^{N_j} E_{ij}^2}$$

where N_j is the number of depth levels for each experiment and E is

$$E_{ij} = \frac{1}{2} (d_{j+1} - d_j) \sqrt{(\text{SE}_{ij}^2 + \text{SE}_{ij+1}^2)}$$

where SE_{ij} ($\text{mg C m}^{-3} \text{ d}^{-1}$) is the standard error for each rate at each depth level.

Bermuda Atlantic Time-series Study (BATS) data—To interpret our results in a regional context, we obtained in situ hydrographic and biogeochemical data from the BATS program for the 1993–2002 period and April to September 2004, which were used in combination with altimetry data for the same periods. Details of the BATS sampling scheme, analytical methods, data quality control, and intercalibration procedures appear in the BATS Methods Manual (Knap et al. 1993). Data are available from the BATS web site at <http://www.bbsr.edu/cintoo/bats/bats.html>.

Table 1. Details of oxygen evolutions experiments carried out during the OC404-1 and OC404-4 cruises in the Sargasso Sea in summer 2004. Numbers in brackets represent CTD stations and dates used to describe hydrographic properties (see Fig. 3).

Cruise	Exp No.	Stn. No.	Location	Position	Date	Depth (m)	PAR	T	CTC	Mean	STD
OC404-1	1	6 (4)	A1	32.67°N, 63.47°W	15 (15) Jun 2004	0	100	24.4			
OC404-1	1	6 (4)	A1	32.67°N, 63.47°W	15 (15) Jun 2004	20	33	23.9			
OC404-1	1	6 (4)	A1	32.67°N, 63.47°W	15 (15) Jun 2004	40	14	24.0			
OC404-1	1	6 (4)	A1	32.67°N, 63.47°W	15 (15) Jun 2004	80	1	21.9	x	21.8	0.3
OC404-1	2	15 (12)	C2	31.18°N, 59.60°W	19 (18) Jun 2004	0	100	23.8			
OC404-1	2	15 (12)	C2	31.18°N, 59.60°W	19 (18) Jun 2004	20	33	23.7			
OC404-1	2	15 (12)	C2	31.18°N, 59.60°W	19 (18) Jun 2004	40	20	22.1	x	22.1	0.2
OC404-1	2	15 (12)	C2	31.18°N, 59.60°W	19 (18) Jun 2004	80	7	18.7	x	19	1
OC404-1	3	20 (18)	C1	30.50°N, 64.92°W	22 (21) Jun 2004	0	100	24.6			
OC404-1	3	20 (18)	C1	30.50°N, 64.92°W	22 (21) Jun 2004	20	33	24.3			
OC404-1	3	20 (18)	C1	30.50°N, 64.92°W	22 (21) Jun 2004	40	20	21.4	x	21.4	0.3
OC404-1	3	20 (18)	C1	30.50°N, 64.92°W	22 (21) Jun 2004	60	7	19.9	x	19.9	0.3
OC404-1	3	20 (18)	C1	30.50°N, 64.92°W	22 (21) Jun 2004	100	1	19.0	x	19.1	0.3
OC404-1	4	63 (40)	C1	30.87°N, 65.33°W	02 Jul (27 Jun) 2004	0	100	27.6			
OC404-1	4	63 (40)	C1	30.87°N, 65.33°W	02 Jul (27 Jun) 2004	25	33	25.0	x	25.0	0.1
OC404-1	4	63 (40)	C1	30.87°N, 65.33°W	02 Jul (27 Jun) 2004	45	20	23.0	x	23.0	0.3
OC404-1	4	63 (40)	C1	30.87°N, 65.33°W	02 Jul (27 Jun) 2004	65	7	20.9	x	21.0	0.2
OC404-1	4	63 (40)	C1	30.87°N, 65.33°W	02 Jul (27 Jun) 2004	115	1	19.0	x	19.1	0.4
OC404-1	5	65	BATS	31.63°N, 64.17°W	03 Jul 2004	0	100	26.3			
OC404-1	5	65	BATS	31.63°N, 64.17°W	03 Jul 2004	20	33	24.1	x	24.0	0.2
OC404-1	5	65	BATS	31.63°N, 64.17°W	03 Jul 2004	40	20	21.4	x	21.4	0.1
OC404-1	5	65	BATS	31.63°N, 64.17°W	03 Jul 2004	90	1	19.1	x	19.0	0.2
OC404-4	6	26	BATS	31.67°N, 64.17°W	30 Jul 2004	0	100	27.9			
OC404-4	6	26	BATS	31.67°N, 64.17°W	30 Jul 2004	20	20	27.8			
OC404-4	6	26	BATS	31.67°N, 64.17°W	30 Jul 2004	40	7	23.9	x	24	1
OC404-4	6	26	BATS	31.67°N, 64.17°W	30 Jul 2004	60	4.5	21.5	x	21.6	0.9
OC404-4	6	26	BATS	31.67°N, 64.17°W	30 Jul 2004	115	1	19.5	x	19.7	0.9
OC404-4	7	50 (7)	C1	30.68°N, 65.77°W	05 Aug (27 Jul) 2004	0	100	27.7			
OC404-4	7	50 (7)	C1	30.68°N, 65.77°W	05 Aug (27 Jul) 2004	30	33	27.6			
OC404-4	7	50 (7)	C1	30.68°N, 65.77°W	05 Aug (27 Jul) 2004	50	20	24.6	x	24.5	0.2
OC404-4	7	50 (7)	C1	30.68°N, 65.77°W	05 Aug (27 Jul) 2004	75	4.5	21.6	x	21.7	0.4
OC404-4	7	50 (7)	C1	30.68°N, 65.77°W	05 Aug (27 Jul) 2004	115	1	19.7	x	19.9	0.8

PAR, photosynthetic active radiation level (%) used for on deck samples incubation; T, temperature in situ; CTC, constant temperature control system; mean, averaged temperature along the experiments; STD, standard deviation. A1 is anticyclonic eddy A1; C2, cyclonic eddy C2; C1, cyclonic eddy C1; BATS, Bermuda Atlantic Time-series site.

Indirect estimates of NCP (NCPe) for the 1993–2002 period were calculated according to

$$\text{NCPe} = {}^{14}\text{C PP} - \text{BCD}$$

where ${}^{14}\text{C PP}$ is the rate of ${}^{14}\text{C}$ incorporation by phytoplankton and BCD is the rate of bacterial carbon demand. BCD was estimated as

$$\text{BCD} = \frac{\text{BG} \times \text{ICF} \times \text{CCF}}{\text{BGE}}$$

where BG is bacterial growth rate measured by the {3H-methyl}-thymidine (${}^3\text{H-TdR}$) technique (Steinberg et al. 2001); ICF and CCF are isotope and carbon conversion factors, respectively; and BGE is the bacterial growth efficiency reported in the literature (see Table 2). PP and BG were integrated down to the base of the euphotic zone at the BATS site (~100 m; Steinberg et al. 2001). Photosynthetic (PQ = 1.4) and respiratory (RQ = 1.1) quotients were assumed in order to transform oxygen to carbon units (Laws 1991; Laws et al. 2000).

There are two important caveats associated with our estimates of NCP. First, the ${}^{14}\text{C}$ assimilation technique

underestimates gross primary production, and, second, estimating respiration on the basis of BCD underestimates total respiration.

The ${}^{14}\text{C}$ technique underestimates gross primary production depending on a variety of factors, including length of the incubation (Karl et al. 1998; Marra 2002; Corno et al. 2006). Studies comparing in vitro O_2 fluxes with ${}^{14}\text{C}$ production rates during JGOFS (Joint Global Ocean Flux Study) cruises determined that ${}^{14}\text{C}$ productivities incubated over 24 h were about 45% of gross carbon production rates calculated from gross O_2 production (Bender et al. 1999; Laws et al. 2000). In contrast to the 24-h incubations used in Bender and Laws studies, BATS ${}^{14}\text{C}$ incubations are dawn-to-dusk. Therefore, BATS ${}^{14}\text{C}$ rates may be closer to gross primary production than the factor of two indicated by Bender and Laws. However, it is not possible to quantify this relationship at BATS because ${}^{14}\text{C}$ and ${}^{18}\text{O}$ methods have not been compared there.

The second caveat to interpretation of NCPe is that estimating respiration on the basis of BCD ignores contributions from other trophic levels that could constitute a significant fraction of the total respiration. Heterotrophic bacteria are considered to be responsible for a large

Table 2. Ranges of parameters values used in the Monte Carlo simulations. ICF is the isotope conversion factor; CCF, carbon conversion factor and BGE, bacterial growth efficiency.

Parameter	Min.	Max.	Units	Source
ICF	0.2	5.6	$\times 10^{18}$ cell mol ⁻¹	Carlson et al. 1996
CCF	3.5	13	fg C cell ⁻¹	Ducklow and Carlson 1992; Christian and Karl 1994; Caron et al. 1995; Carlson and Ducklow 1996; Carlson et al. 1996; Zubkov et al. 2000; Fukuda et al. 2002; Gundersen et al. 2002
BGE	7	19	%	Carlson and Ducklow 1996

fraction of the total respiration, particularly in the least productive areas (Williams 1981). Del Giorgio and Duarte (2002) reviewed the current information on the contribution of various biotic components and depth layers to respiration in the open ocean, and they assumed that zooplankton respiration represents 5% of the combined microplankton respiration in the photic and thermocline waters. Roman et al. (2002) estimated mesozooplankton production at BATS site to be 2% of primary production at this site. Using heterotrophic microplankton biomass data from Caron et al. (1995) (0.95 $\mu\text{g C L}^{-1}$) and the averaged weight-specific respiration rate for flagellates and ciliates published in Caron et al. (1990) (5.5×10^{-6} nL O₂ μm^{-3} h⁻¹), we estimate heterotrophic microplankton respiration for the Sargasso Sea to be ~ 40 mg C m⁻² d⁻¹. This number is one order of magnitude lower than our estimation of bacteria carbon demand (see below). On this basis, we assumed bacterial remineralization to represent the main contribution to total respiration.

Unfortunately, it is not possible to quantify the errors associated with underestimation of gross primary production by the ¹⁴C assimilation technique and underestimation of respiration by BCD in computation of NCPe and thereby assess the absolute accuracy of the NCPe estimates. However, to the extent that these systematic errors remain constant over time, we can interpret NCPe as a proxy for variability in NCP.

A Monte Carlo procedure was used to incorporate the uncertainty in the parameters and conversion factors

mentioned above into our calculations of NCPe and BCD. For each iteration, parameter values were drawn at random from their probability distributions. PP and BG were assumed to be normally distributed with means and standard deviations computed from the BATS dataset for 1993–2002 (Table 3). Variability, both within and between cruises conducted on a given month of the year, was incorporated into these calculations. Values for ICF, CCF, and BGE were drawn from uniform distributions with limits defined by values reported in the literature (Table 2). Ten thousand iterations were used to obtain an empirical probability distribution of NCPe and BCD. Finally, we computed the probability of autotrophy for each month as the ratio between the number of iterations with NCPe > 0 and the total number of iterations.

Results

Eddy trajectories and sea-level anomaly (SLA) history—

The three candidate eddies: anticyclone A1 and cyclones C1 and C2, were tracked in the satellite data archive to determine their trajectories and recent history of sea-level anomaly extrema (Fig. 2). Retrospective analysis of sea-level anomaly suggested a remote origin for A1 at approx. 40°N, 40°W in April 2003 (data not shown). In June 2004, A1 was a persistently strong feature located north of BATS, at approx. 33.5°N, 62.7°W, with sea-level anomaly extremum greater than 20 cm.

Table 3. Computed monthly averaged rates (mg C m⁻² d⁻¹) of ¹⁴C incorporation by phytoplankton (¹⁴C PP), bacterial growth (BG), bacterial carbon demand (BCD), and estimated net community production (NCPe), integrated to the 1% light depth (100 m) for the period from 1993 to 2002. STD is standard deviation; *p* statistic probability for BATS site to be in net autotrophic balance.

Month	¹⁴ C PP		BG		BCD		NCPe		<i>p</i> (NCPe>0)
	Mean	STD	Mean	STD	Mean	STD	Mean	STD	
Jan	373	153	62	52	293	378	72	417	0.67
Feb	465	137	50	17	238	205	225	246	0.84
Mar	531	252	60	22	289	251	246	356	0.78
Apr	499	363	94	67	446	519	47	622	0.59
May	462	207	98	65	479	529	-11	566	0.59
Jun	365	112	94	25	449	365	-82	380	0.50
Jul	477	178	126	72	605	616	-120	655	0.53
Aug	348	152	95	56	446	458	-105	498	0.51
Sep	356	81	71	50	340	390	17	400	0.64
Oct	378	112	57	31	274	275	105	298	0.72
Nov	346	168	47	27	223	231	122	289	0.72
Dec	366	159	42	18	198	183	164	244	0.78
Ann. rate	46	87	70	9	336	78	382	37	

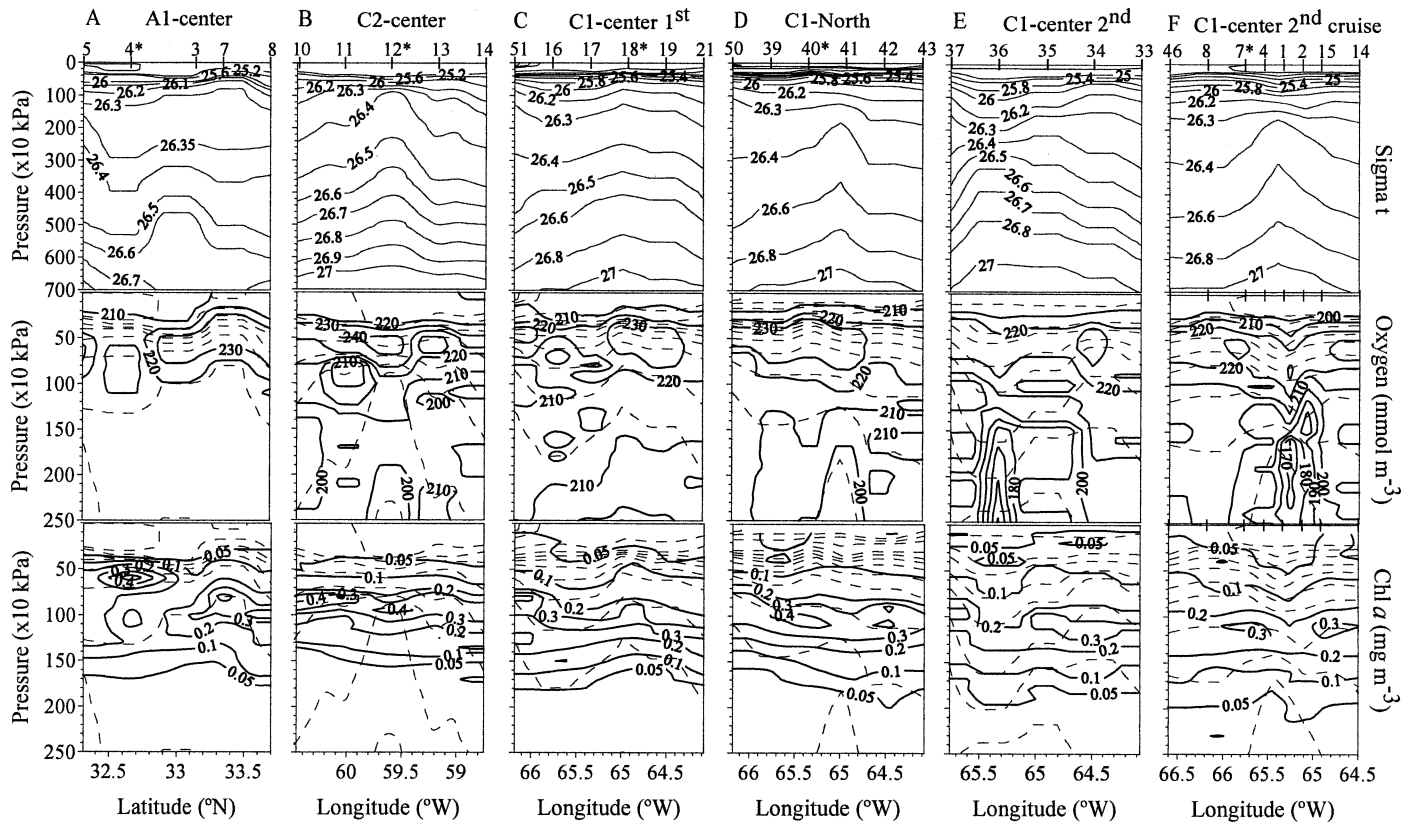


Fig. 4. Vertical distribution of sigma-t, oxygen concentration, and Chl *a* concentration across eddies (A) A1, (B) C2, and (C) C1. (D) Northern CTD section across the C1 eddy during the first cruise; (E) second reoccupation of the C1-center section (C), three days later. (F) Central CTD section across C1 eddy during the second cruise. Dashed lines printed over oxygen and chlorophyll plots represent sigma-t distribution. Numbers on the top axis represent CTD station numbers. The asterisks indicate stations where net community production (NCP) experiments were carried out.

In June 2004, sea-level anomalies associated with C1 and C2 were centered at 30.5°N, 64.7°W and 31.3°N, 60.5°W, respectively. Retrospective analysis of the sea-level anomaly archive showed that both cyclonic eddies had originated from the same feature that split in two in late March 2004. C1 intensified significantly during May 2004, during which time its edge affected BATS site and reached a sea-level anomaly extremum greater than 225 cm in June 2004. Between the first and second cruise (June–August 2004), C1 moved westward (approx. 31.0°N, 65.6°W) and was associated with a less intense sea-level anomaly. C2 fluctuated within a 10–20 cm extremum from the time of its split with C1 through the period of observations.

Hydrographic structure and mesoscale variability in metabolic balance—The vertical thermal structure across A1 revealed a bolus of 26.5 sigma-t and 16°C water (Fig. 4A), as opposed to the thick lens of 18°C water characteristic of mode water eddies in this region (McGillcuddy et al. 1999). A 1500 m cast at the center of A1 (data not shown) indicated depression of the main pycnocline of several hundred meters. The depression of the main pycnocline is responsible for the positive sea-level anomaly associated with A1 (Fig. 1) and its overall anticyclonic rotation (data not shown). A relative increase in oxygen

concentration ($>230 \text{ mmol m}^{-3}$) was observed in the upper $80 \times 10 \text{ kPa}$ north from eddy center and also at the southern periphery. The deep chlorophyll maximum (DCM), typically located at $\sim 100 \times 10 \text{ kPa}$ in the surrounding waters, shoaled to $\sim 60 \text{ m}$ at station 4, where Chl *a* concentration was $>0.5 \text{ mg m}^{-3}$. However, when this station was reoccupied seven hours later and samples for the NCP experiment were collected, the DCM ($\sim 0.4 \text{ mg m}^{-3}$) was located at $\sim 110 \times 10 \text{ kPa}$ (Fig. 5). Such rapid fluctuations could indicate small-scale spatial variability or the presence of internal wave packets, which have been reported as a common feature in the Sargasso Sea (Eriksen 1988) and are associated with high subsurface chlorophyll concentrations in large mesoscale features (Granata et al. 1995).

The CTD section across C2 (Fig. 4B) revealed a clear upward perturbation of both the seasonal and main pycnoclines. The 26.4 isopycnal shoaled $\sim 200 \times 10 \text{ kPa}$ over horizontal scales of $\sim 80 \text{ km}$. Although sigma-t at $100 \times 10 \text{ kPa}$ resembled that of deeper layers, sigma-t at $50 \times 10 \text{ kPa}$ was quite patchy, and the sense of sigma-t at $5 \times 10 \text{ kPa}$ was nearly opposite to those of the deeper layers. A mesoscale peak in oxygen concentration ($>240 \text{ mmol m}^{-3}$) was observed at the eddy center at $\sim 60 \times 10 \text{ kPa}$. The distribution of Chl *a* concentration was more homo-

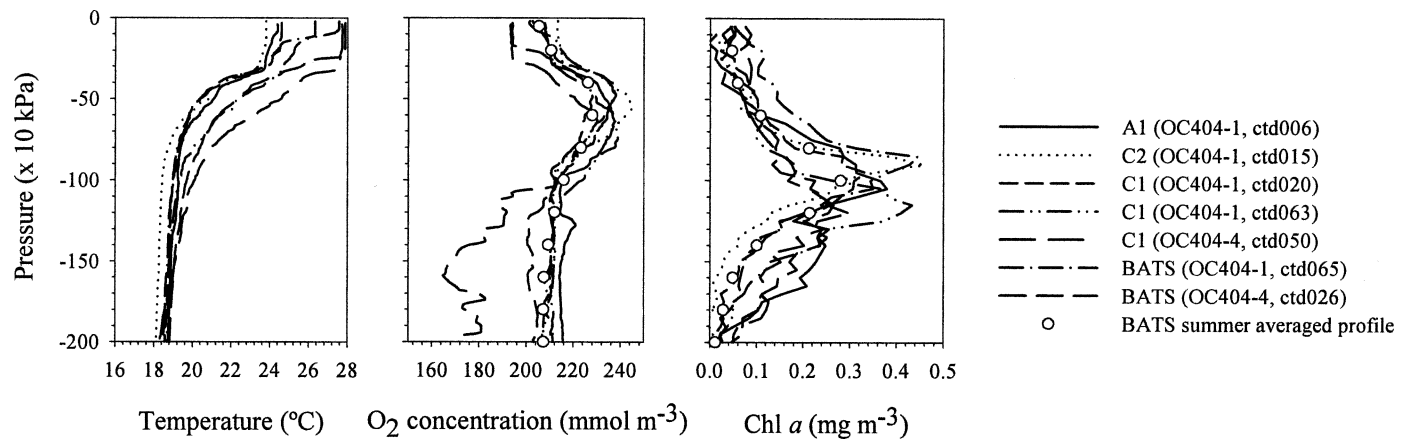


Fig. 5. Profiles of temperature, oxygen concentration, and Chl *a* in the upper 200 × 10 kPa at A1 (CTD 6, first cruise), C2 (CTD 15, first cruise), C1 (CTD 20, first cruise), C1 (CTD 63, first cruise), C1 (CTD 50, second cruise), and BATS site (CTD 65, first cruise, and CTD 26, second cruise). Circles correspond to summer averages calculated for the BATS site from the 1993–2002 data sets.

geneous than observed in A1. Slightly higher Chl *a* concentrations ($>0.45 \text{ mg m}^{-3}$) were measured at stations 12 and 11.

Two E-W sections through the center of C1 during the first cruise (Fig. 4C,D) revealed its impact on the main pycnocline as well as on the upper ocean properties. The 26.4 isopycnal shoaled more than $80 \times 10 \text{ kPa}$ over horizontal scales of $\sim 80 \text{ km}$. Oxygen concentration in excess of 230 mmol m^{-3} was observed at the eddy center (stations 18 and 19) in the first section (Fig. 4C) and in the western part of the northern CTD section at $\sim 50 \times 10 \text{ kPa}$ (Fig. 4D). The DCM resided at 110 m, which was slightly deeper than at C2. Higher Chl *a* concentrations ($>0.45 \text{ mg m}^{-3}$) were observed at the western periphery of the eddy (station 51), where the DCM shoaled $\sim 20 \times 10 \text{ kPa}$, in the southern section (Fig. 4C), and at both sides of the eddy center (stations 42 and 40) in the northern CTD section (Fig. 4D). A small spatial scale feature, missed on the first occupation of the transect through the center of C1 (Fig. 4C), was observed when this transect was reoccupied three days later (Fig. 4E). The vertical hydrographic structure showed shoaling of the main pycnocline and deepening of the seasonal pycnocline associated with thinning of the 18°C water mass. The subsurface maximum in dissolved oxygen at $\sim 50 \text{ m}$ weakened between the first and second occupations. Moreover, the second transect revealed a large subsurface minimum in dissolved oxygen ($<145 \text{ mmol m}^{-3}$) at $\sim 300 \text{ m}$. Chl *a* at the eddy center decreased, and the minimum chlorophyll was located one station west of the eddy center (station 36).

Based on the information provided by the CTD sections across the eddies, measurements of net oxygen production and respiration were conducted at stations influenced by eddy activity, where relatively enhanced fluorescence was observed. The metabolic balance of the photic layer was also studied at BATS site, initially chosen as a background reference station for summer conditions. Unfortunately, no experiments were conducted on the second occupation of the transect through the center of C1 (Fig. 4E), where the large subsurface minimum in dissolved oxygen was observed at $\sim 300 \text{ m}$. The vertical distribution of NCP, R,

and GPP rates at the edge of A1 (station 4, see Fig. 4), center of C2 (station 12) and C1 (station 18), northern edge of C1 (station 40), and BATS site, during the first cruise is shown in Figure 6. During the first cruise, only the experiment carried out at A1 yielded negative NCP estimates ($<-0.5 \text{ mmol O}_2 \text{ m}^{-3} \text{ d}^{-1}$) at all depths where the experiment was performed, consistent with relatively high respiration rates ($>0.8 \text{ mmol O}_2 \text{ m}^{-3} \text{ d}^{-1}$). NCP rates were positive in the upper $40 \times 10 \text{ kPa}$ at C1 and C2, and decreased to almost zero further down. Maximum values of NCP were found at the surface in the center of C2 and C1, although NCP at the surface of C2 ($1.6 \pm 0.1 \text{ mmol O}_2 \text{ m}^{-3} \text{ d}^{-1}$) was four times higher than at C1 ($0.35 \pm 0.5 \text{ mmol O}_2 \text{ m}^{-3} \text{ d}^{-1}$). In the northern section across C1, the maximum NCP value was found at $25 \times 10 \text{ kPa}$ ($0.4 \pm 0.3 \text{ mmol O}_2 \text{ m}^{-3} \text{ d}^{-1}$). At BATS site, high values of NCP ($>3.0 \text{ mmol O}_2 \text{ m}^{-3} \text{ d}^{-1}$) were measured in the upper $90 \times 10 \text{ kPa}$.

Depth-integrated rates revealed significant differences between the eddies (Fig. 7A). During the first cruise, A1 exhibited negative NCP ($-73 \pm 14 \text{ mmol O}_2 \text{ m}^{-2} \text{ d}^{-1}$) and relatively high R ($112 \pm 19 \text{ mmol O}_2 \text{ m}^{-2} \text{ d}^{-1}$). The highest depth-integrated NCP rates were obtained for C2 ($34 \pm 7 \text{ mmol O}_2 \text{ m}^{-2} \text{ d}^{-1}$) and BATS ($48 \pm 5 \text{ mmol O}_2 \text{ m}^{-2} \text{ d}^{-1}$). Low values of NCP ($<8 \text{ mmol O}_2 \text{ m}^{-2} \text{ d}^{-1}$) were found at C1, which exhibited relatively high values of R ($60 \pm 15 \text{ mmol O}_2 \text{ m}^{-2} \text{ d}^{-1}$) in the experiment carried out north of the eddy center.

Temporal changes at C1 and the BATS site—Because of the small spatial scale feature observed across C1 during the first cruise, the resolution of stations in the eddy core was increased during the second cruise (Fig. 4F). The E-W section through the eddy center during the second cruise showed a similar vertical hydrographic structure observed during the second occupation of the eddy center as that observed during the first cruise, although some evolution was evident (Fig. 4E). The depression of the upper seasonal pycnocline at eddy center appeared to have relaxed somewhat with respect to the first cruise. A band of $>220 \text{ mmol m}^{-3}$ oxygen concentration was observed at 60

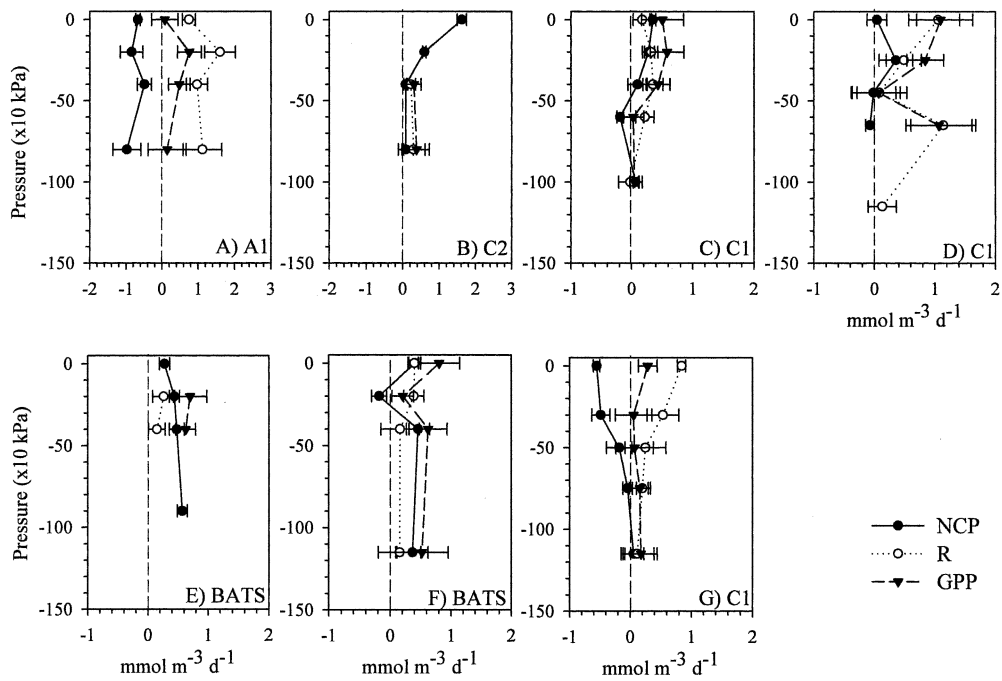


Fig. 6. Profiles of net community production (NCP), respiration (R), and gross primary production (GPP) rates at (A) A1 edge, (B) C2 center, (C) C1 center, (D) C1 northern edge and BATS site, (E) during the first cruise, and (F) BATS site, and (G) C1 edge in the central section during the second cruise.

$\times 10$ kPa along the E-W CTD section. This layer of high oxygen concentration was located deeper at the eddy center ($\sim 80 \times 10$ kPa). The oxygen deficit observed during the first cruise at 300×10 kPa was still present at eddy center, but it had shoaled somewhat and become less intense ($< 170 \text{ mmol m}^{-3}$). The DCM was located at $\sim 110 \times$

10 kPa. Chl *a* concentrations were lower than those observed during the first cruise.

During the second cruise, the metabolic balance was measured one station west of the C1 inner core, where relatively enhanced Chl *a* concentrations were observed (Fig. 4F). Dramatic changes between the first and the

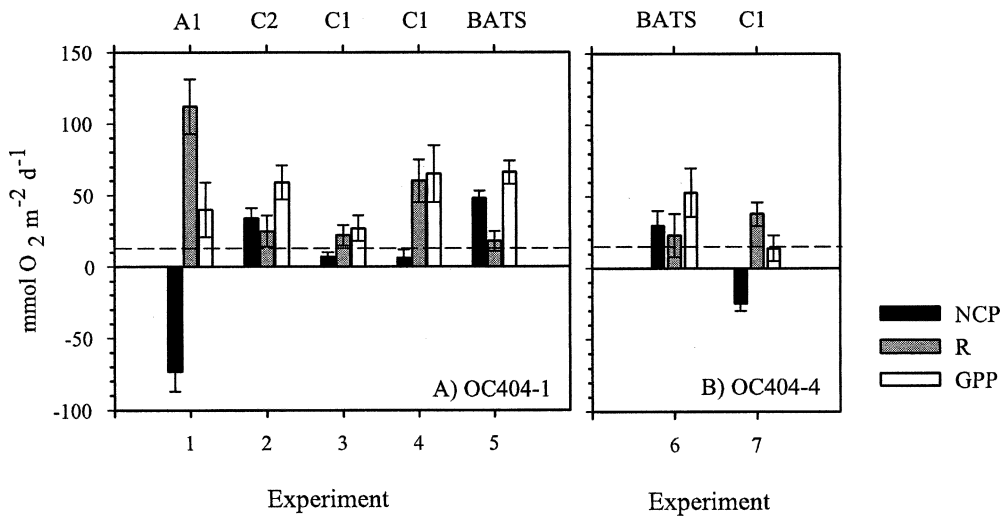


Fig. 7. Depth-integrated net community production (NCP), respiration (R), and gross primary production rates (GPP) measured (A) at the edge of A1 (exp. 1), C2 center (exp. 2), C1 center (exp. 3), C1 northern edge (exp. 4) and BATS site (exp. 5), during the first cruise, and (B) BATS site (exp. 6) and C1 edge in the central section (exp. 7) during the second cruise. Depth integrations were calculated down to the photic layer depth (~ 100 m). Dashed line represents the annual new production ($\sim 50 \text{ g C m}^{-2} \text{ yr}^{-1}$) estimated by Jenkins and Goldman (1985) and converted to oxygen units assuming a $PQ = 1.4$.

Table 4. Depth-integrated values of oxygen concentration, Chl *a*, net community production (NCP), respiration (R), and gross primary production (GPP) at selected stations. CTD station numbers are shown in brackets. Values in the last column correspond to averaged summer conditions computed from the 1993–2002 BATS data set.

Variable	Units	OC404-1 cruise						OC404-4 cruise						Summer 1993–2001 BATS					
		A1 (CTD 4, 6)		C2 (CTD 12, 15)		C1 (CTD 18, 20)		C1 (CTD 40, 63)		C1 (CTD 36)		BATS (CTD 65)		BATS (CTD 26)		C1 (CTD 7, 49, 50)			
		Mean	SE	Mean	SE	Mean	SE	Mean	SE	Mean	SE	Mean	SE	Mean	SE	Mean	SE		
O ₂ (0–100 m)	mmol O ₂ m ⁻²	20765	± 1103	22142	± 27	22190	± 210	22405	± 104	21352		21826		20980		20660	± 186	20926	± 1427
Chl <i>a</i> (0–150 m)	mg m ⁻²	28	± 1	20	± 1	22.7	± 0.4	27	± 4	18		29		22		20	± 1	25	± 9
NCP (100 m)	mmol O ₂ m ⁻² d ⁻¹	-73	± 14	34	± 7	7	± 3	6	± 6			48	± 5	30	± 10	-25	± 5		
R (100 m)	mmol O ₂ m ⁻² d ⁻¹	112	± 19	25	± 11	22	± 7	60	± 15			18	± 7	23	± 15	58	± 8		
GPP (100 m)	mmol O ₂ m ⁻² d ⁻¹	40	± 19	59	± 12	27	± 9	65	± 20			66	± 8	53	± 17	14	± 9		

second cruises were observed in the upper 40 × 10 kPa, where a decrease to negative values (< -0.5 mmol O₂ m⁻³ d⁻¹) was observed in NCP rates (Fig. 6). Depth-integrated rates showed a shift from net autotrophy to net heterotrophy in the metabolic balance of the photic layer (Fig. 7B). The decrease in NCP rates associated with C1 was consistent with the reduction of oxygen concentration in the photic layer observed between cruises (Table 4). The in situ O₂ balance (-14 ± 10 mmol O₂ m⁻² d⁻¹) computed for the upper 100 m, using the oxygen concentration integrated down to the photic layer and the time elapsed between cruises (six weeks), compares well with the in vitro oxygen balance computed from the NCP rates measured at C1 (-9 mmol O₂ m⁻² d⁻¹). This agreement between the in situ oxygen balance and the direct measurements of NCP is to some degree fortuitous, as physical processes such as gas exchange can contribute net fluxes on the same order as the observed change in oxygen inventory (Musgrave et al. 1988).

The vertical profiles carried out at BATS site showed deepening of the isotherms in the upper 200 × 10 kPa between cruises (Fig. 5). Associated with these changes, the oxygen concentration in the photic layer decreased (see also Table 4) and the DCM was located deeper and associated with lower Chl *a* values (~0.3 mg m⁻³). NCP rates at the BATS site decreased to negative values (-0.2 ± 0.1 mmol O₂ m⁻³ d⁻¹) at 20 × 10 kPa (Fig. 6F), and a slight decrease was observed in NCP rates integrated to the base of the euphotic layer (Fig. 7).

Averaged summer values of oxygen and Chl *a* concentration computed from the 1993–2002 BATS data set are shown in Table 4. The data reported across the eddies and BATS site during OC404-1 and OC404-4 cruises compare well with these climatologies.

Discussion

Direct NCP measurements for summer 2004—Our results show a high variability in the metabolic balance associated with mesoscale eddies. The type and age of an eddy appear to be important factors controlling the observed variability. For example, a net heterotrophic balance of the photic layer and relatively high respiration rates were observed at A1, an anomalous 16°C MWE with a remote origin at approx. 40°N, 40°W in April 2003. Based on MODIS imagery (data not shown), the relative high values of Chl *a* concentration observed in A1 could be associated with a streamer spiraling inward toward the eddy center. Enhanced chlorophyll concentration and respiration rates have been associated with anticyclonic eddies in the Canary Islands region (Aristegui and Montero 2005). These authors proposed that anticyclonic eddies may entrain high-chlorophyll water from upwelling filaments with which they interact. NCP rates measured in C2 in June 2004 were approximately five times higher than in C1 (see Table 4). A comparison of hydrographic information obtained at the centers of both eddies showed that the uplifting of isotherms in the upper 200 × 10 kPa was more intense at C2 (Fig. 4). Higher oxygen concentration values were associated with C2 in the upper 100 × 10 kPa (Fig. 5).

Although no large differences in Chl *a* concentration were observed between C2 and C1, the DCM was in general shallower at C2. These observations suggest that more intense pumping of nutrients into the surface layers could have been taking place at C2. Deepening sea-level anomaly in C2 over time also indicates that the feature was intensifying, as opposed to C1, which appeared to be in a decay phase (data not shown).

The hydrographic data also show changes through the center of C1 between the first and second cruise (Fig. 4). These changes in the hydrographic structure of C1 coincided with the decrease in intensity of the subsurface minimum in oxygen concentration observed between 150 and 400×10 kPa, a decrease in Chl *a* concentration, and the shift in the metabolic balance at the center of the eddy, which changed from net autotrophic to net heterotrophic. Although we can not discard the idea that some of the temporal changes observed in the metabolic balance associated with C1 were associated with imperfect sampling of a small-scale feature during the first cruise, these data suggest that, at the time we sampled C1 during the second cruise, the eddy was in a late state of decaying biological response.

Whereas the NCP differences between eddies and the temporal changes observed in C1 are consistent with prior expectations based on eddy age (Sweeney et al. 2003), the measurements at BATS site, initially chosen as our background reference station for summer conditions, remain enigmatic. Two possible scenarios can be invoked to interpret these results: (1) NCP estimates at BATS constitute good reference points for summer conditions, and the mesoscale eddies sampled in this study contained NCP comparable to the background level, or (2) NCP estimates at the BATS site are enhanced with respect to background summer conditions, and the magnitude of the enhancement is similar to that observed in association with eddy-driven upwelling. Therefore, the background conditions must be determined in order to distinguish between the two scenarios proposed above.

Variability in NCP background conditions: NCPe estimates from BATS data—Whilst a relatively extensive database of phytoplankton photosynthetic carbon assimilation exists for subtropical regions (Steinberg et al. 2001; Teira et al. 2005), the laborious and time-consuming estimation of NCP and R rates has severely hampered the development of a regional database (Serret et al. 2002). This situation is particularly acute for the Sargasso Sea, where, to our knowledge, only one direct estimate of NCP has been reported so far, describing a net heterotrophic balance of the surface waters in summertime (-0.7 ± 0.1 mmol O₂ m⁻³ d⁻¹; Williams and Jenkinson 1982).

The lack of an extensive set of direct NCP estimates for this region makes it challenging to interpret our results. However, several different estimates of net production provide valuable information about seasonal patterns in the balance between photosynthesis and respiration in this region. By studying the seasonal cycle of oxygen supersaturation, Jenkins and Goldman (1985) estimated photosyn-

thetic production to be of the order of 0.5 mmol m⁻² d⁻¹, consistent with a net autotrophic metabolic balance through the year. Serret et al. (pers. comm.) used a predictive model for NCP, based on an empirical relationships with ¹⁴C-derived primary production rates, to find seasonal alternations of net autotrophic and net heterotrophic conditions, which could lead to an annually compensated metabolic balance at BATS site in the upper 200 m. Using the observed variability of the ¹³C: ¹²C ratio for the same region, Gruber et al. (pers. comm.) estimated positive values for NCP during almost the entire year, with maximum values found in late spring. From a nine year study carried out at BATS, Steinberg et al. (2001) reported higher primary production (PP) than bacterial carbon demand (BCD) values in winter and spring-bloom events, with a tight coupling of BCD and PP in the summer. Some periods in the time series wherein BCD exceeds PP were ascribed to a greater portion of gross primary production partitioned as dissolved organic carbon, or to an over-estimation of BCD due to the use of an inappropriately low bacterial growth efficiency coefficient.

We studied the seasonal variability in the balance between photosynthesis and respiration at BATS by estimating monthly averages of NCP (NCPe) for the 1993–2002 period, computed as the difference between ¹⁴C PP and BCD (see Methods section). There was high variability in the ¹⁴C PP values (Fig. 8), with maximum monthly averages found in March (531 mg C m⁻² d⁻¹) associated with the spring bloom. Second-to-largest mean values were found for July (477 mg C m⁻² d⁻¹). Detailed analysis of hydrographic and moored data highlights the role of mesoscale activity on the extreme values observed in July 1995, a period during which a mode water eddy was present at BATS (McNeil et al. 1999). BCD was maximum from April to September, after the spring bloom. The maximum averaged monthly value was found in July (~ 700 mg C m⁻² d⁻¹). The variability in BCD and NCPe values spanned in general the variability of available direct observations of dark community respiration and net community production from in vitro changes in dissolved oxygen experiments. NCPe monthly values, which were not significantly different from zero, were always positive except in the summer months. The statistical probability of BATS site to be in net autotrophic balance is higher than 0.5 through the year (see Table 3). Our estimate of the annual net community production in the photic layer (1 ± 3 mol C m⁻²) is lower than the values reported by Jenkins and Goldman (1985; ~ 3.4 mol C m⁻²) and Gruber et al. (1998; ~ 2.3 mol C m⁻²). These differences could be attributed, at least partially, to the fact that our NCPe analyses did not include the production of dissolved organic matter by phytoplankton, which can be significant, particularly in oligotrophic regions (Karl et al. 1998; Teira et al. 2001).

The pattern in NCPe values we found for BATS contrasts with results obtained for station ALOHA, in the oligotrophic North Pacific (Williams et al. 2004), where respiration tends to exceed photosynthesis throughout the year. Although we do not have seasonal coverage in direct NCP measurements, it is interesting to note that the direct

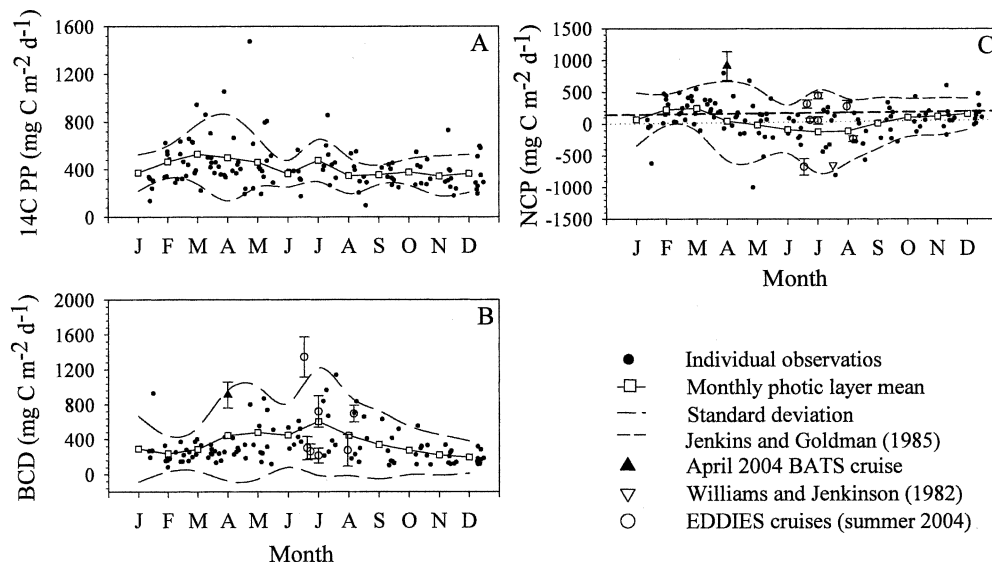


Fig. 8. Monthly means of (A) ^{14}C incorporation rates by phytoplankton (^{14}C PP), (B) bacterial carbon demand (BCD), and (C) net community production (NCPe) estimated for the 1993–2002 period at the BATS site. Black dots represent individual observational points, with values of BCD and NCPe computed using the best-guess parameter set. White squares are monthly means integrated to the 1% light depth (100 m) (see Table 3). Medium dashed line represents standard deviations about the monthly means, for BCD and NCPe derived from the Monte Carlo analysis. Long dashed line represents the annual new production estimated for the region by Jenkins and Goldman (1985). NCP rates estimated from in vitro changes in dissolved oxygen after 24-h incubations in the BATS region are also indicated.

NCP observations described here are consistent with the Karl et al.'s (2003) hypothesis of autotrophy in the open ocean being episodic. However, unlike the constancy in heterotrophic processes proposed by Karl et al. (2003), our analyses show that total variability in BCD (coefficient of variation, CV, 65%) is higher than that of PP rates (CV = 56%) (Fig. 8). These results suggest that episodic pulses of net autotrophy at BATS sites could be explained, at least partially, by variability in respiration processes. The idea of pulses in net autotrophy being generated by a reduction in respiration rates is consistent with recent observations of net autotrophic balances associated with cyclonic eddies in the NE Atlantic (Gonzalez et al. 2001; Maixandeau et al. 2005), and ascribed to a relative reduction in respiration rates.

Mechanisms responsible for enhanced NCP rates at BATS in summer 2004—Our direct NCP observations suggest that averaged metabolic balance reported for the summer months is the result of highly variable NCP rates associated with mesoscale eddies. To investigate the influence of processes that could be responsible for the enhanced NCP rates found at BATS in the summer of 2004, we studied the temporal evolution of temperature and Chl *a* at BATS from April to September 2004 (Fig. 9). Vertical sections showed an uplifting of the isotherms in the upper 200×10 kPa at the time this station was occupied during the OC404-1 and OC404-4 cruises. The Chl *a* distribution showed that the deep chlorophyll maximum was slightly shallower during the first EDDIES cruise (OC404-1) (see also vertical profiles in Fig. 5). Sea-level anomaly data

from altimeter images indicated that in early and late July, when NCP experiments were carried out at BATS, this station could have been under the influence of subsurface processes associated with interaction of A1 and C1. Unfortunately, we cannot resolve subsurface processes with the data set available in this study. However, a combination of altimeter and hydrographic data from the time series at BATS provides valuable information as to a potential link between enhanced NCP rates and eddy-eddy interactions. Figure 10 shows NCPe anomalies for 1993–2002, which were computed with respect to monthly averages (see Table 3) and rescaled to values between zero and 10. Colored bars indicate periods under the influence of cyclonic (blue), anticyclonic (red), and mode water eddies (yellow). NCP anomalies were considered unusually large when they were greater than an arbitrary threshold of 2.5 in our 1–10 scale (i.e., 25% of the largest value). Seven of these large NCPe anomalies occurred in periods when BATS was under the influence of mesoscale eddies. Analysis of the altimeter images for 1993–2002 reveals that nine other events of large NCP anomalies were associated with eddy-eddy interactions (green) and therefore were potentially influenced by the input of nutrients into the photic layer driven by subsurface processes. The 1993–2002 retrospective analyses indicate that, although subjected to an important interannual variability, most of the time, BATS was under the influence of cyclonic and anticyclonic eddies, meanders, or eddy-eddy interactions.

A number of studies (Martin and Richards 2001; Sanchez and Gil 2004) have already suggested that a better understanding of the biogeochemical impacts of subme-

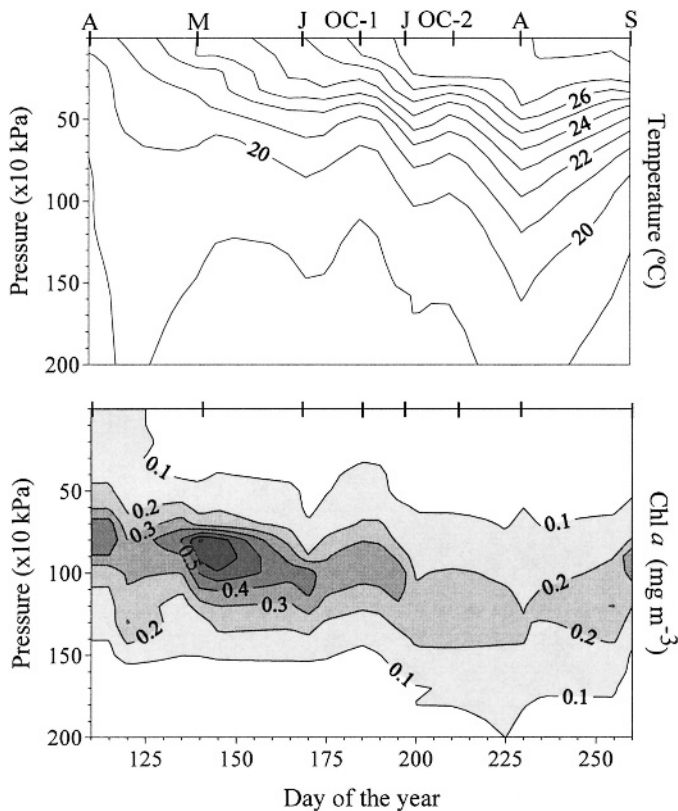


Fig. 9. Temporal evolution in the vertical distribution of (A) temperature, and (B) Chl *a* from April 2004 to September 2004 at BATS site. OC404-1 (OC-1) and OC404-4 (OC-2) cruises are indicated.

scale processes is needed. Clearly, hydrographic information with a higher spatial and temporal resolution is needed to resolve the connections between our NCP results and mesoscale/submesoscale processes. Our results, however, suggest that in the summer of 2004, BATS site was under the influence of eddy-eddy interactions (corresponding to the second scenario above) and that NCP rates were relatively enhanced at BATS and in the cyclonic eddy C2.

An important caveat to this interpretation is that it is difficult to assess background conditions that are not influenced by mesoscale dynamics. This region is populated by closely packed eddies that are constantly evolving and interacting with each other (Fig. 1). As such, we do not have negative controls with which to compare our direct NCP measurements in eddies, and therefore cannot unequivocally diagnose the influence of mesoscale effects. In our view, the only way to do so would be to obtain a long-term time series of direct NCP measurements together with targeted observations in mesoscale features. Only with background conditions defined by the long-term seasonal mean will it be possible to distinguish between the variety of processes that contribute to the net metabolic balance at this site.

Direct NCP observations carried out in three mesoscale eddies investigated in the Sargasso Sea in the summer of 2004 ranged from negative to positive values, and the age and type of the sampled eddy were important factors responsible for this variability. Positive rates occurred in younger cyclones and in areas of eddy-eddy interactions, whereas negative NCP rates were observed in anticyclones and older cyclone features in the process of decay. Indirect NCP estimates obtained by difference of ^{14}C phytoplankton production and bacterial carbon demand rates from the

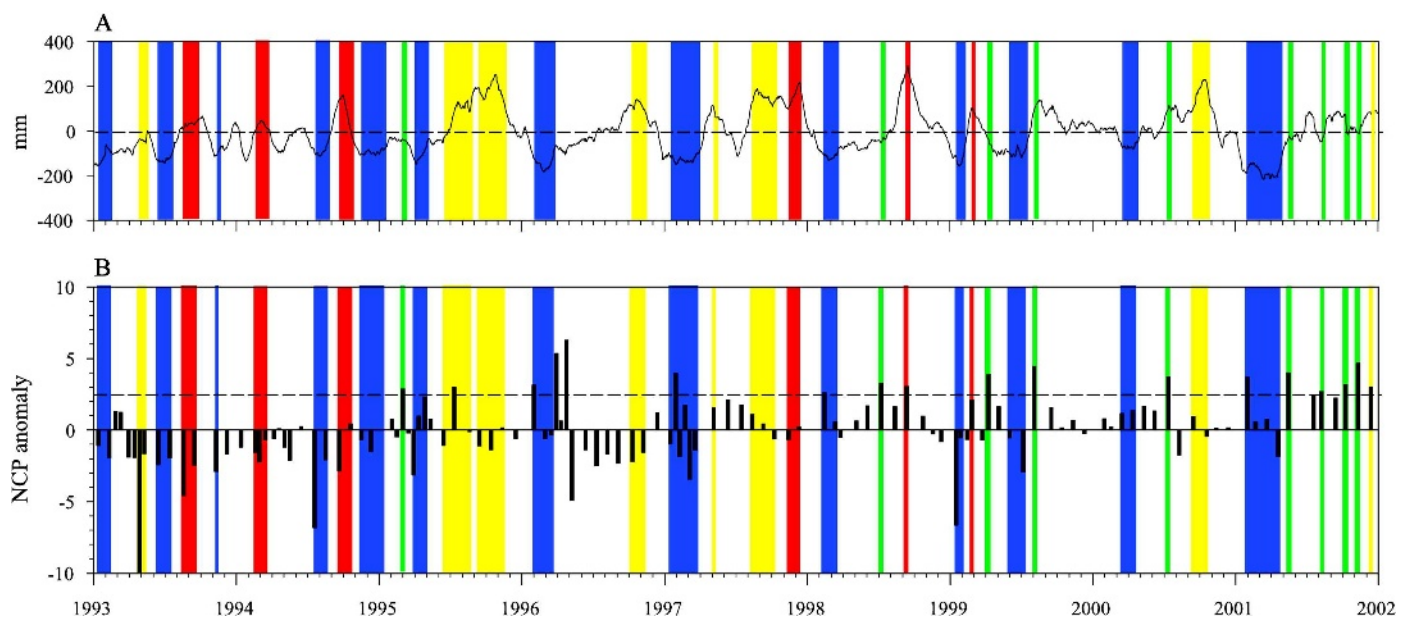


Fig. 10. (A) Sea-level anomalies (SLA) estimated for the 1993–2002 period at the BATS site. (B) Net community production (NCPe) anomalies for 1993–2002 computed with respect to monthly averages and rescaled to values between 1 and 10. Colored bars indicate periods under the influence of cyclonic (blue), anticyclonic (red), mode water eddies (yellow), and eddy-eddy interactions (green).

BATS time-series were highly variable and spanned the range of direct NCP observations. Although our indirect NCP estimates are low compared to other estimates for the region (Table 6 in Gruber et al. 1998), they provide a context in which to interpret variability in direct NCP observations.

A more extensive set of direct observations would be needed to resolve the annual balance between photosynthesis and respiration and to quantify the integrated effect of eddies at this oligotrophic subtropical site. However, our results reveal that the metabolic balance in this area is subject to a wide range of temporal and spatial scales of variability in both photosynthesis and respiration processes. NCP rates measured during the EDDIES cruises were up to three times the annual new production estimated for the region (Jenkins and Goldman 1985) (Fig. 7), supporting the hypothesis that episodic events of net autotrophy can contribute substantially to the long-term metabolic balance of subtropical regions (Karl et al. 2003).

In spite of the remarkable effort and success of time-series programs like BATS or HOT, the temporal and spatial variability of mechanisms that force and control biological responses is only partially resolved by the relative monthly temporal sampling. In this regard, future work should be aimed at understanding the effect of higher-frequency, smaller-scale variability in the processes controlling the metabolic balance of planktonic communities, which is crucial in order to comprehend the role of the upper ocean in regulating air-sea fluxes of CO₂.

References

- ARISTEGUI, J., AND M. F. MONTERO. 2005. Temporal and spatial changes in plankton respiration and biomass in the Canary Islands region: The effect of mesoscale variability. *J. Marine Syst.* **54**: 65–82.
- BENDER, M., J. ORCHARDO, M. L. DICKSON, R. BARBER, AND S. LINDLEY. 1999. In vitro O₂ fluxes compared with C-14 production and other rate terms during the JGOFS Equatorial Pacific experiment. *Deep-Sea Res. Pt. I* **46**: 637–654.
- CARLSON, C. A., AND H. W. DUCKLOW. 1996. Growth of bacterioplankton and consumption of dissolved organic carbon in the Sargasso Sea. *Aquat. Microb. Ecol.* **10**: 69–85.
- , ———, AND T. D. SLEETER. 1996. Stocks and dynamics of bacterioplankton in the northwestern Sargasso Sea. *Deep-Sea Res. Pt. II* **43**: 491–515.
- CARON, D. A., J. C. GOLDMAN, AND T. FENCHEL. 1990. Protozoan respiration and metabolism, p. 307–322. *In* G. M. Capriolo [ed.], *Ecology of marine protozoa*. Oxford Univ. Press.
- , AND OTHERS. 1995. The contribution of microorganisms to particulate carbon and nitrogen in surface waters of the Sargasso Sea near Bermuda. *Deep-Sea Res. Pt. I* **42**: 943–972.
- CHRISTIAN, J. R., AND D. M. KARL. 1994. Microbial community structure at the United States Joint Global Ocean Flux Study Station Aloha—inverse methods for estimating biochemical indicator ratios. *J. Geophys. Res.-Oceans* **99**: 14269–14276.
- CORNO, G., R. LETELIER, M. ABBOTT, AND D. KARL. 2006. Assessing primary production variability in the North Pacific Subtropical Gyre: a comparison of fast repetition rate fluorometry and ¹⁴C measurements. *J. Phycol.* **42**: 51–60.
- DEL GIORGIO, P. A., AND C. M. DUARTE. 2002. Respiration in the open ocean. *Nature* **420**: 379–384.
- DUARTE, C. M., S. AGUSTÍ, P. A. DEL GIORGIO, AND J. J. COLE. 1999. Regional carbon imbalances in the oceans. *Response. Science* **284**: 1735b.
- DUCKLOW, H. W., AND C. A. CARLSON. 1992. Oceanic bacterial production. *Adv. Microb. Ecol.* **12**: 113–181.
- ERIKSEN, C. C. 1988. Variability in the upper-ocean internal wave field at a Sargasso Sea site. *J. Phys. Oceanogr.* **18**: 1495–1513.
- FERNANDEZ, E., AND OTHERS. 2004. The spatial distribution of plankton communities in a Slope Water anticyclonic Oceanic eDDY (SWODDY) in the southern Bay of Biscay. *J. Mar. Biol. Assoc. UK* **84**: 501–517.
- FUKUDA, R., O. HIROSHI, T. NAGATA, AND I. KOIKE. 2002. Direct determination of carbon and nitrogen contents of natural bacterial abundance assemblages in marine environments. *Appl. Environ. Microb.* **64**: 3352–3358.
- GONZALEZ, N., AND OTHERS. 2001. The metabolic balance of the planktonic community in the North Atlantic Subtropical Gyre: The role of mesoscale instabilities. *Limnol. Oceanogr.* **46**: 946–952.
- GRANATA, T., J. WIGGERT, AND T. DICKEY. 1995. Trapped, near-inertial waves and enhanced chlorophyll distributions. *J. Geophys. Res.-Oceans* **100**: 20793–20804.
- GRUBER, N., C. D. KEELING, AND T. F. STOCKER. 1998. Carbon-13 constraints on the seasonal inorganic carbon budget at the BATS site in the northwestern Sargasso Sea. *Deep-Sea Res. Pt. I* **45**: 673–717.
- GUNDERSEN, K., M. HELDAL, S. NORLAND, D. A. PURDIE, AND A. H. KNAP. 2002. Elemental C, N, and P cell content of individual bacteria collected at the Bermuda Atlantic Time-series Study (BATS) site. *Limnol. Oceanogr.* **47**: 1525–1530.
- JENKINS, W. J., AND J. C. GOLDMAN. 1985. Seasonal oxygen cycling and primary production in the Sargasso Sea. *J. Mar. Res.* **43**: 465–491.
- KARL, D. M., D. V. HEBEL, K. BJORKMAN, AND R. M. LETELIER. 1998. The role of dissolved organic matter release in the productivity of the oligotrophic North Pacific Ocean. *Limnol. Oceanogr.* **43**: 1270–1286.
- , E. A. LAWS, P. MORRIS, P. J. L. WILLIAMS, AND S. EMERSON. 2003. Global carbon cycle—metabolic balance of the open sea. *Nature* **426**: 32.
- KNAP, A. H., AND OTHERS. 1993. BATS methods manual, Version 3. U.S. JGOFS Planning Office.
- LAWS, E. A. 1991. Photosynthetic quotients, new production and net community production in the open ocean. *Deep-Sea Res.* **38**: 143–167.
- , M. R. LANDRY, R. T. BARBER, L. CAMPBELL, M. L. DICKSON, AND J. MARRA. 2000. Carbon cycling in primary production bottle incubations: Inferences from grazing experiments and photosynthetic studies using C-14 and O-18 in the Arabian Sea. *Deep-Sea Res. Pt. II* **47**: 1339–1352.
- MAIXANDEAU, A., AND OTHERS. 2005. Microbial community production, respiration, and structure of the microbial food web of an ecosystem in the northeastern Atlantic Ocean. *J. Geophys. Res.-Oceans* **110**, C07S17, doi:10.1029/2004JC002694.
- MARRA, J. 2002. Approaches to the measurement of plankton production, p. 78–108. *In* P. J. L. Williams, D. N. Thomas and C. S. Reynolds [eds.], *Phytoplankton productivity: Carbon assimilation in marine and freshwater ecosystems*. Blackwell Publ. Ltd.
- MARTIN, A. P., AND K. J. RICHARDS. 2001. Mechanisms for vertical nutrient transport within a North Atlantic mesoscale eddy. *Deep-Sea Res. Pt. II* **48**: 757–773.

- MCGILLICUDDY, D. J., R. JOHNSON, D. A. SIEGEL, A. F. MICHAELS, N. R. BATES, AND A. H. KNAP. 1999. Mesoscale variations of biogeochemical properties in the Sargasso Sea. *J. Geophys. Res.-Oceans* **104**: 13381–13394.
- , AND A. R. ROBINSON. 1997. Eddy-induced nutrient supply and new production in the Sargasso Sea. *Deep-Sea Res. Pt. I* **44**: 1427–1450.
- MCNEIL, J. D., H. W. JANNASCH, T. DICKEY, D. MCGILLICUDDY, M. BRZEZINSKI, AND C. M. SAKAMOTO. 1999. New chemical, bio-optical and physical observations of upper ocean response to the passage of a mesoscale eddy off Bermuda. *J. Geophys. Res.-Oceans* **104**: 15537–15548.
- MOURINO, B., E. FERNANDEZ, R. PINGREE, B. SINHA, J. ESCANEZ, AND D. DE ARMAS. 2005. Constraining effect of mesoscale features on carbon budget of photic layer in the NE subtropical Atlantic. *Mar. Ecol. Prog. Ser.* **287**: 45–52.
- MUSGRAVE, D. L., J. CHOU, AND W. J. JENKINS. 1988. Application of a model of upper-ocean physics for studying seasonal cycles of oxygen. *J. Geophys. Res.-Oceans* **93**: 15679–15700.
- NEUER, S., AND OTHERS. 2002. Differences in the biological carbon pump at three subtropical ocean sites. *Geophys. Res. Lett.* **29**, 1885, doi:10.1029/2002GL015393.
- ROBINSON, C., AND OTHERS. 2002. Plankton respiration in the eastern Atlantic Ocean. *Deep-Sea Res. Pt. I* **49**: 787–813.
- ROMAN, M. R., H. A. ADOLF, M. R. LANDRY, L. P. MADIN, D. K. STEINBERG, AND X. ZHANG. 2002. Estimates of oceanic mesozooplankton production: A comparison using the Bermuda and Hawaii time-series data. *Deep-Sea Res. Pt. II* **49**: 175–192.
- SANCHEZ, R., AND J. GIL. 2004. 3D structure, mesoscale interactions and potential vorticity conservation in a swoddy in the Bay of Biscay. *J. Mar. Syst.* **46**: 47–68.
- SERRET, P., E. FERNANDEZ, AND C. ROBINSON. 2002. Biogeographic differences in the net ecosystem metabolism of the open ocean. *Ecology* **83**: 3225–3234.
- SIEGEL, D. A., D. J. MCGILLICUDDY, AND E. A. FIELDS. 1999. Mesoscale eddies, satellite altimetry, and new production in the Sargasso Sea. *J. Geophys. Res.-Oceans* **104**: 13359–13379.
- STEINBERG, D. K., C. A. CARLSON, N. R. BATES, R. J. JOHNSON, A. F. MICHAELS, AND A. H. KNAP. 2001. Overview of the U.S. JGOFS Bermuda Atlantic Time-series Study (BATS): A decade-scale look at ocean biology and biogeochemistry. *Deep-Sea Res. Pt. II* **48**: 1405–1447.
- SWEENEY, E. N., D. J. MCGILLICUDDY, AND K. O. BUESSELER. 2003. Biogeochemical impacts due to mesoscale eddy activity in the Sargasso Sea as measured at the Bermuda Atlantic Time-series Study (BATS). *Deep-Sea Res. Pt. II* **50**: 3017–3039.
- TEIRA, E., M. J. PAZO, P. SERRET, AND E. FERNANDEZ. 2001. Dissolved organic carbon production by microbial populations in the Atlantic Ocean. *Limnol. Oceanogr.* **46**: 1370–1377.
- , AND OTHERS. 2005. Variability of chlorophyll and primary production in the eastern North Atlantic Subtropical Gyre: Potential factors affecting phytoplankton activity. *Deep-Sea Res. Pt. I* **52**: 569–588.
- WILLIAMS, P. J. L. 1981. Microbial contribution to overall marine plankton metabolism: Direct measurements of respiration. *Oceanol. Acta* **4**: 359–364.
- . 1998. The balance of plankton respiration and photosynthesis in the open oceans. *Nature* **394**: 55–57.
- , AND N. W. JENKINSON. 1982. A transportable microprocessor-controlled precise Winkler titration suitable for field station and shipboard use. *Limnol. Oceanogr.* **27**: 576–584.
- , P. J. MORRIS, AND D. M. KARL. 2004. Net community production and metabolic balance at the oligotrophic ocean site, station ALOHA. *Deep-Sea Res. Pt. I* **51**: 1563–1578.
- ZUBKOV, M. V., M. A. SLEIGH, P. H. BURKILL, AND R. J. G. LEAKEY. 2000. Bacterial growth and grazing loss in contrasting areas of North and South Atlantic. *J. Plank. Res.* **22**: 685–711.

Received: 18 November 2005

Accepted: 13 June 2006

Amended: 29 July 2006